Structure of the high-spin, β-decaying state in the neutron-rich nucleus ^{146}La

S. Lalkovski,[1,2] F. G. Kondev,[2] K. Auranen,[2,*] A. D. Ayangeakaa,[3,4] M. P. Carpenter,[2] J. A. Clark,[2,5] P. Copp,[2] N. P. Giha,[6] D. J. Hartley,[7] T. Lauritsen,[2] S. Marley,[8] G. E. Morgan,[8] C. Müller-Gatermann,[2] S. Nandi,[2] W. Reviol,[2] D. Santiago-Gonzalez,[2] G. Savard,[2,9] D. Seweryniak,[2] Ir. B. Vasilev,[1] and J. Wu[2,†]

[1]*Faculty of Physics, Sofia University "St. Kliment Ohridski", Sofia 1164, Bulgaria*
[2]*Physics Division, Argonne National Laboratory, Lemont, Illinois 60439, USA*
[3]*Department of Physics and Astronomy, University of North Carolina, Chapel Hill, North Carolina 27599, USA*
[4]*Triangle Universities Nuclear Laboratory, Duke University, Durham, North Carolina 27708, USA*
[5]*Department of Physics and Astronomy, University of Manitoba, Winnipeg, Manitoba R3T 2N2, Canada*
[6]*Department of Nuclear Engineering and Radiological Sciences, University of Michigan, Ann Arbor, Michigan 48109, USA*
[7]*Department of Physics, U.S. Naval Academy, Annapolis, Maryland 21402, USA*
[8]*Department of Physics and Astronomy, Louisiana State University, Baton Rouge, Louisiana 70803, USA*
[9]*Department of Physics, University of Chicago, Chicago, Illinois 60637, USA*

(Received 5 June 2023; accepted 16 January 2024; published 8 February 2024)

Excited structures in ^{146}Ce were populated in β decay of the high-spin state in the neutron-rich nucleus ^{146}La. The beam was produced by the Californium Rare Isotope Breeder Upgrade (CARIBU) facility at Argonne National Laboratory, reaccelerated by the ATLAS accelerator, and implanted on a moving-tape system in the middle of the GAMMASPHERE array. The decay scheme of the high-spin, β-decaying state in ^{146}La was revised with respect to previous studies and evaluated nuclear data. The structure of ^{146}La is discussed in the framework of the deformed Nilsson model and systematics of known quasiparticle structures in the region.

DOI: 10.1103/PhysRevC.109.024309

I. INTRODUCTION

The neutron-rich ^{146}La nucleus ($Z = 57$, $N = 89$) is located in the region near $Z = 56$–58 and $N = 88$–92 that has been predicted for a long time to exhibit octupole-deformed shapes [1,2]. Experimental evidences were found for the existence of such shapes in the neighboring ^{144}Ba [3] and ^{146}Ba [4] nuclei.

Spectroscopic information on the structure of ^{146}La is summarized in the latest ENSDF evaluation [5] and in two more recent publications [6,7]. Two β-decaying states, one of low spin and shorter half-life [$J^\pi = (2^-)$, $T_{1/2} = 6.1(3)$ s] and the other of higher spin and longer half-life [$J^\pi = (6^-)$, $T_{1/2} = 9.8(4)$ s], are established in ^{146}La, with the former proposed to be the ground state [5]. Recently, high-precision Canadian Penning Trap (CPT) mass measurements established the energy difference between the two β-decaying states as 141.5 (24) keV [8], but their ordering is still elusive.

The decay properties of the two β-decaying states in ^{146}La are of interest to the nuclear structure [9–11] and nuclear astrophysics [12,13] communities, as well as to nuclear applications, such as decay heat from nuclear reactors and antineutrino spectra reconstructions [14]. Several studies are reported in the literature (see Ref. [5] and reference therein), but they are far from complete since the lifetimes of the two β-decaying states are similar and it was difficult to separate their decays using a moving-tape detection system.

In the present work, we report on β-γ-γ and γ-γ-γ coincidence studies of the high-spin, β-decaying state in ^{146}La. The new results extended the decay scheme and resolved ambiguities that existed from previous studies. The structure of ^{146}La is discussed using the deformed Nilsson model and systematics of known quasiparticle structures in neighboring nuclei.

II. EXPERIMENTAL SETUP AND DATA ANALYSIS

A. β-γ-γ experiment

The neutron-rich ^{146}La nuclei were produced by the Californium Rare Isotope Breeder Upgrade (CARIBU) facility [15] at Argonne National Laboratory (ANL). The beam was reaccelerated by the Argonne Tandem Linear Accelerator System (ATLAS) and implanted onto a 0.5-in.-wide Mylar moving tape that was coated with iron oxide. The implantation point was surrounded by an array of six plastic scintilator detectors, known as HExagonal ARray for Triggering (HEART) [16], which was used to detect β particles produced in the decay of ^{146}La. The system was located in the center of the GAMMASPHERE spectrometer, comprising 62 Compton-suppressed high-purity germanium HPGe detectors for this experiment. Energy and efficiency calibrations of the array

*Present address: Accelerator Laboratory, Department of Physics, University of Jyväskylä, FI-40014 Jyväskylä, Finland.

†Present address: National Nuclear Data Center, Brookhaven National Laboratory, Upton, New York 11973, USA.

were carried out using ^{56}Co, ^{152}Eu, ^{182}Ta, and ^{243}Am sources. The moving-tape cycle selected in the present experiment was tailored to the known half-lives of the two β-decaying states [5]. It began with a 2-s-long background measurement, where no incoming beam was present (beam off), followed by a 60-s implantation (beam on) period and by a 100-s beam-off period, where the decays of the implanted nuclei were measured. After that, the tape moved and the long-lived activity was transported away from the array, followed by 2-s background measurement. Collected data were sorted into various one- and two-dimensional histograms using the GEBSORT software [17] and the analysis was carried out with the ROOT [18] and RADWARE [19] computer programs.

B. γ-γ-γ experiment

Additional GAMMASPHERE data, where γ rays were produced by a stationary 34.4-μCi ^{252}Cf source placed in the center of the array, were also used as a cross reference in the present analysis. These data were collected continuously for about 30 days and details about the experiment can be found in Ref. [20]. The events were sorted into a three-dimensional histogram and they were analysed using the LEVIT8R program from the RADWARE computer package [19].

Gamma rays from prompt-fission and beta-decaying fragments were present in the collected data as the fission products were stopped within the source. However, the former are in coincidence with γ rays emitted by the complementary fission fragments (e.g., $^{102-104}$Zr in the case of ^{146}Ce), while such correlations are lost in the delayed spectra owing to the long β-decay half-lives. As a consequence, γ rays detected without the observation of complementary fission fragments are most likely only emitted during the β-decay process. In addition, β decays of neutron-rich nuclei often proceed via non-yrast levels, which are usually not populated in the prompt-fission process, thus providing additional distinction. Nevertheless, the data from this experiment were a mixture of prompt and delayed γ rays; the triple coincidences registered by GAMMASPHERE proved beneficial in establishing many weak transitions produced in the decay of the high-spin β-decaying state in ^{146}La.

III. EXPERIMENTAL RESULTS

Prior to the present work, β-decay spectroscopy studies of the two isomers in ^{146}La, including β-γ-γ angular correlations, were carried out at the TRISTAN (BNL) [21–23] and KUR-ISOL (Kyoto) [24,25] facilities, as summarized in the most-recent ENSDF evaluation [5]. Excited structures in the daughter nucleus ^{146}Ce were also studied in spontaneous fission of ^{252}Cf and in neutron-induced fission of ^{235}U, where the ground state and octupole bands were observed up to spins of (10^+) [26] and (15^-) [27], respectively.

The present work is built on the existing knowledge and revises the previously known decay scheme of the high-spin, β-decaying state in ^{146}La. It also confirms the existence of two β-decaying states, as shown in Fig. 1. The half-lives of 9.9(1) and 6.1(2) s obtained in the present study are in a good agreement with the previously measured values (see Ref. [5] and references therein), but have a higher precision.

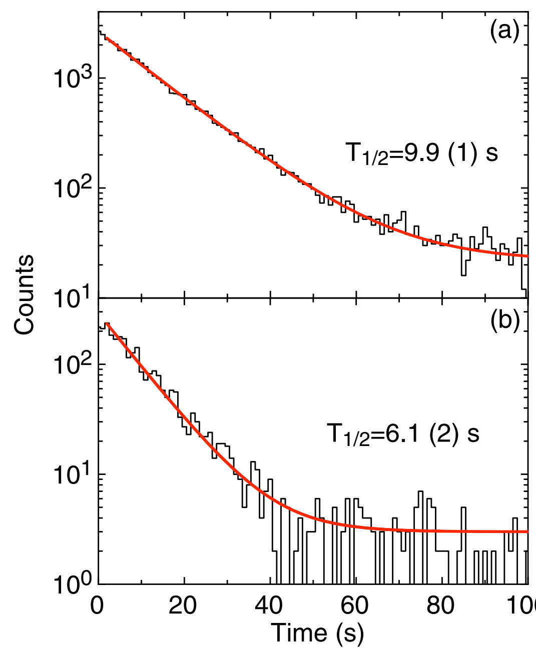

FIG. 1. Time spectra produced by gating on (a) 410-, 503- and 515-keV γ rays, depopulating the 4^+, 6^+, and 5^- levels at 669-, 1172-, and 1184-keV, respectively; (b) the 925-keV γ ray, depopulating the 1^- level at 925 keV. The solid lines represent least-squares fits using a single-exponential decay and a constant background.

A partial level scheme of the high-spin, β-decaying state in ^{146}La showing only states up to 2 MeV is presented in Fig. 2. Sample γ-ray spectra are presented in Figs. 3 and 4. The measured γ-ray energies and relative intensities are listed in Table I, where the quoted spin and parity assignments are taken from Ref. [5], except for the 1770-, 1893-, and 1956-keV levels, which were redefined in the present work based on the observed γ-ray deexcitation patterns. In addition, the present observation do not support the $J^\pi = (6^+)$ and (4^+) assignments proposed in Ref. [5] for the levels at 2271 and 2415 keV, respectively. The reported β-decay feeding intensities in Table I were determined from the proposed decay scheme and intensity balance considerations. The log ft values were calculated using the LOGFT program [28] and $Q_\beta(^{146}\text{La}) = 6405(15)$ keV, as recommended in AME2020 [29].

Since the half-lives of the two β-decaying states are similar, it was not possible to unambiguously separate their decays using the moving-tape system. Instead, differences in γ-ray multiplicities and, as a consequence, distinctive γ-ray deexcitation patterns, were used to discriminate events associated with decays of the high-spin and the low-spin β-decaying states. In the data analysis, we initially investigated γ-ray transitions that directly feed the 4^+ level at 669 keV, the 5^- level at 1184 keV, and the 6^+ level at 1172 keV, which enabled placement of states with $J \geqslant 4$ in the level scheme. After that, we studied γ-ray decay branches to the lower-spin states.

TABLE I. Level energies, spins and parities, β-decay feeding intensities, log ft values, γ-ray energies and relative intensities for the levels observed in the β decay of the $K^{\pi}=5^-$ state in ^{146}La.

E_i (keV)	J^{π} [a] ($\hbar$)	I_β (%)	log ft	E_γ (keV)	I_γ (rel. units)	E_f (keV)
0.0	0^+					
258.7(5)	2^+			258.7(5)	1000(8)	0.0
668.5(6)	4^+	12.5(17)	6.59(9)	409.8(5)	937(19)	258.7(5)
961.1(6)	3^-			292.5(5)	7.4(8)	668.5(6)
				702.3(5)	69(6)	258.7(5)
1171.5(6)	6^+	5.5(8)	6.76(7)	503.1(5)	231(5)	668.5(6)
1183.5(6)	5^-	5.5(9)	6.75(8)	514.7(5)	288(6)	668.5(6)
1274.9(6)	2^+			314(1)	0.4(2)	961.1(6)
				1016(1)	5.7(2)	258.7(5)
				1275(1)	2.1(9)	0.0
1550.8(6)	7^-	$\leqslant 4.1$ [c]	$\geqslant 6.7$	366.8(5)	29.5(25)	1183.5(6)
				379.7(5)	68(4)	1171.5(6)
1627.5(6)	4^+	10.0(12)	6.33(6)	353(1)	4.3(7)	1274.9(6)
				444.3(5)	15.1(15)	1183.5(6)
				666.2(5)	28(4)	961.1(6)
				958.5(5)	118(10)	668.5(6)
				1369.2(5)	35.7(29)	258.7(5)
1691.8(12)		1.8(3)	7.05(8)	141(1)	12.4(17)	1550.8(6)
1712.1(6)	(5^-) [b]	3.9(3)	6.70(4)	162(1)	0.62(22)	1550.8(6)
				527(1)	8.4(15)	1183.5(6)
				750.9(5)	15.0(20)	961.1(6)
				1044.0(5)	17.9(20)	668.5(6)
1737.1(9)	8^+			187(1)	1.0(4)	1550.8(6)
				565(1)	1.8(4)	1171.5(6)
1747.8(12)		1.42(20)	7.13(7)	197(1)	12.9(18)	1550.8(6)
1770.1(7)	$(4, 5^-)$ [b]	2.2(3)	6.93(6)	809.1(5)	22.5(22)	961.1(6)
				1102(1)	3.4(18)	668.5(6)
1810.7(6)	5^+	10.7(10)	6.22(5)	183.5(5)	61(4)	1627.5(6)
				627.5(5)	10.4(16)	1183.5(6)
				639.1(5)	24.9(20)	1171.5(6)
				1142.0(5)	71.5(31)	668.5(6)
1877.1(12)	$(4, 5^-)$	0.81(16)	7.32(9)	916(1)	8.7(17)	961.1(6)
1892.4(7)	$(4, 5, 6^+)$ [b]	2.0(3)	6.92(7)	123(1)	1.6(9)	1770.1(7)
				708.5(5)	10.0(19)	1183.5(6)
				1224.2(5)	17.3(21)	668.5(6)
1917.1(12)	$(4, 5^-)$	0.17(7)	7.98(21)	956(1)	1.8(8)	961.1(6)
1956.3(7)	$(5^-, 6^+)$ [b]	2.9(12)	6.73(18)	405(1)	6.7(8)	1550.8(6)
				773.3(5)	23.1(20)	1183.5(6)
				784.9(5)	11.8(17)	1171.5(6)
				1288(1)	9.3(20)	668.5(6)
2032.0(6)	(4^+)	3.2(4)	6.66(6)	757(1)	3.9(20)	1274.9(6)
				861(1)	6.8(16)	1171.5(6)
				1363.8(5)	10.2(20)	668.5(6)
				1772.6(7)	14.1(23)	258.7(5)
2066.1(9)		1.06(15)	7.12(7)	515(1)	4.4(6)	1550.8(6)
				895(1)	7.1(14)	1171.5(6)
2090.4(8)	$(4^+, 5, 6^+)$ [b]	1.9(3)	6.86(7)	907(1)	2.7(5)	1183.5(6)
				918(1)	6.1(17)	1171.5(6)
				1422.6(9)	11.7(21)	668.5(6)
2130.2(8)		1.97(22)	6.82(5)	948(1)	1.6(5)	1183.5(6)
				959(1)	8.4(11)	1171.5(6)
				1460.5(9)	11.3(20)	668.5(6)
2140.5(9)	$(4^+, 5, 6)$ [b]	1.05(15)	7.09(7)	957(1)	4.5(7)	1183.5(6)
				969(1)	6.8(14)	1171.5(6)
2177.6(7)	$(4^+, 5, 6^+)$ [b]	4.6(4)	6.43(4)	366.8(5)	15.9(27)	1810.7(6)

TABLE I. (*Continued.*)

E_i (keV)	J^{π} [a] ($\hbar$)	I_β (%)	log ft	E_γ (keV)	I_γ (rel. units)	E_f (keV)
				550.0(5)	17.8(20)	1627.5(6)
				1007(1)	8.1(18)	1171.5(6)
				1509(1)	7.7(21)	668.5(6)
2185.5(12)		0.58(12)	7.33(9)	1014(1)	6.3(13)	1171.5(6)
2194.5(12)		0.14(4)	7.94(13)	1011(1)	1.5(4)	1183.5(6)
2220.5(12)		0.12(3)	8.00(11)	1049(1)	1.3(3)	1171.5(6)
2231.5(12)		0.21(5)	7.75(11)	1060(1)	2.3(5)	1171.5(6)
2256.9(7)	$(5^-, 6)$[b]	6.9(8)	6.22(5)	301(1)	7.7(12)	1956.3(7)
				446.4(5)	52(8)	1810.7(6)
				706(1)	1.6(7)	1550.8(6)
				1073.1(5)	12.9(16)	1183.5(6)
2262.2(7)		⩽2.9	⩾6.7	307(1)	⩽24	1956.3(7)
				1078.2(5)	30(3)	1183.5(6)
				1090(1)	9.0(18)	1171.5(6)
2270.5(12)	$(4, 5, 6^+)$[b]	0.72(21)	7.20(13)	1602(1)	7.8(22)	668.5(6)
2275.0(9)		0.69(11)	7.22(7)	1091(1)	5.4(11)	1183.5(6)
				1104(1)	2.0(4)	1171.5(6)
2373.5(12)		0.7(3)	7.16(19)	1190(1)	8(3)	1183.5(6)
2396.2(9)		0.53(7)	7.27(6)	846(1)	1.2(2)	1550.8(6)
				1212(1)	4.5(7)	1183.5(6)
2415.3(8)	$(5^-, 6)$[b]	1.12(15)	6.94(6)	523(1)	6.9(14)	1892.4(7)
				864(1)	0.72(12)	1550.8(6)
				1232(1)	4.5(8)	1183.5(6)
2422.5(12)		0.18(4)	7.73(10)	1239(1)	1.9(4)	1183.5(6)
2467.5(12)		0.19(6)	7.69(14)	1296(1)	2.1(6)	1171.5(6)
2488.5(12)		0.43(9)	7.32(10)	1305(1)	4.6(9)	1183.5(6)
2502.5(12)		0.19(4)	7.67(10)	1319(1)	2.0(4)	1183.5(6)
2517.5(12)		0.65(20)	7.13(14)	1849(1)	7.0(21)	668.5(6)
2548.5(12)		0.19(4)	7.65(10)	1365(1)	2.1(4)	1183.5(6)
2580.1(14)		0.093(19)	7.94(9)	843(1)	1.0(2)	1736.5(12)
2609.7(9)		0.30(5)	7.42(8)	1059(1)	1.0(2)	1550.8(6)
				1426(1)	2.2(5)	1183.5(6)
2632.1(14)		0.025(6)	8.49(11)	895(1)	0.27(6)	1737.1(9)
2639.8(12)		0.18(8)	7.63(20)	1089(1)	1.9(8)	1550.8(6)
2649.7(9)		0.24(5)	7.50(9)	1098(1)	0.8(2)	1550.8(6)
				1467(1)	1.8(4)	1183.5(6)
2656.7(9)		0.19(5)	7.59(12)	1106(1)	0.9(4)	1550.8(6)
				1473(1)	1.1(2)	1183.5(6)
2724.5(12)		0.18(4)	7.59(10)	1541(1)	1.9(4)	1183.5(6)
2727.5(12)		0.17(4)	7.61(11)	1544(1)	1.8(4)	1183.5(6)
2751.1(14)		0.024(6)	8.45(11)	1014(1)	0.26(6)	1737.1(9)
2827.1(14)		0.030(6)	8.31(9)	1090(1)	0.32(6)	1737.1(9)
2875.5(12)		0.19(5)	7.48(12)	1692(1)	2.1(5)	1183.5(6)
2914.5(8)		4.3(13)	6.11(14)	652.0(5)	42(14)	2262.2(7)
				1364(1)	1.3(5)	1550.8(6)
				1732(1)	3.1(6)	1183.5(6)
2954.5(12)		0.102(19)	7.71(9)	1771(1)	1.1(2)	1183.5(6)
2982.5(12)		0.111(19)	7.66(8)	1799(1)	1.2(2)	1183.5(6)
2986.5(12)		⩽0.14	⩾7.6	1803(1)	⩽1.9	1183.5(6)
2990.2(9)		0.30(5)	7.23(8)	1439(1)	0.8(2)	1550.8(6)
				1807(1)	2.4(5)	1183.5(6)
3054.5(12)		0.19(4)	7.39(10)	1871(1)	2.1(4)	1183.5(6)
3064.5(12)		0.15(3)	7.49(9)	1881(1)	1.7(3)	1183.5(6)
3066.5(12)		0.14(3)	7.52(10)	1883(1)	1.6(3)	1183.5(6)
3190.5(12)		0.25(6)	7.19(11)	2007(1)	2.7(6)	1183.5(6)
3208.5(12)		0.17(4)	7.35(11)	2025(1)	1.8(4)	1183.5(6)

TABLE I. (*Continued.*)

E_i (keV)	J^π [a] ($\hbar$)	I_β (%)	log ft	E_γ (keV)	I_γ (rel. units)	E_f (keV)
3243.5(12)		0.36(7)	7.01(10)	2060(1)	3.9(8)	1183.5(6)
3422.8(12)		0.08(4)	7.55(22)	1872(1)	0.9(4)	1550.8(6)
3450.2(9)		0.55(10)	6.70(8)	1899(1)	0.4(1)	1550.8(6)
				2267(1)	5.5(10)	1183.5(6)
3471.8(12)		0.046(19)	7.76(19)	1921(1)	0.5(2)	1550.8(6)
3502.2(9)		0.19(4)	7.13(10)	1951(1)	0.5(2)	1550.8(6)
				2319(1)	1.5(3)	1183.5(6)
3532.5(12)		0.37(8)	6.82(10)	2349(1)	4.0(8)	1183.5(6)
3917.5(12)		0.17(4)	6.90(11)	2734(1)	1.8(4)	1183.5(6)
4254.8(12)		0.021(5)	7.55(11)	2704(1)	0.23(5)	1550.8(6)

[a]From ENSDF [5], unless otherwise stated.
[b]Redefined in the present work.
[c]The observed apparent β-decay feeding presumably due to pandemonium.

As can be seen from Table I, the 6^+ level at 1172 keV, the 5^- at 1184 keV, the 4^+ at 1628 keV, and the 5^+ at 1811 keV in ^{146}Ce are among the strongest that are directly fed from the high-spin β-decaying state in ^{146}La, thus restricting the spin of the latter to $J = 5$. The negative parity is proposed in the present work, based on the expected configurations, as discussed in Sec. IV. This assignment is in disagreement with the adopted J$^\pi$ = (6$^-$) in ENSDF [5], which was partially based on the β-decay feeding pattern from Ref. [24] and shell-model arguments. However, the ENSDF value is inconsistent with the observed direct β feedings to several levels with $J^\pi = 4^+$ (see Table I for details), since such transitions would be first-forbidden unique ($\Delta J = 2$, $\Delta\pi = -1$) and one would expect that they are more retarded. It is worth noting, however, that the previous β-decay studies [24] were not able to completely exclude other possible assignments, including the $J^\pi = (5^-)$ proposed here.

Above the 4^+ level at 669 keV, only two lower-spin levels were observed in the present study: the 3^- member of the octupole band at 961 keV and the 2^+ level at 1275 keV (see Fig. 2). The former is fed by several week γ rays originating from 4^+ and $(4, 5^-)$ levels, while the latter is populated by the weak 353- and 757-keV γ-ray transitions depopulating the 1628-keV, 4^+ and 2032-keV, (4^+) levels, respectively. Besides these two levels, none of the low-spin states, associated in Ref. [24] with the β decay of the high-spin state in ^{146}La, can be confirmed in the present study. In particular, the 925-keV transition is observed in the present work to exhibit a half-life consistent with the lower-spin, β-decaying state in ^{146}La [see Fig. 1(b)]. This is in contradiction with the findings of Ref. [24], wherein the $J^\pi = 1^-$ member of the octupole band is reported to be populated via the β decay of the higher-spin state. In addition, we were unable to confirm a number of other weakly populated levels, and corresponding γ rays, reported in Ref. [24].

The 1551-keV level was assigned $J^\pi = 5^-$ in Ref. [24] where it was proposed to depopulate via the 380- and 883-keV transitions. However, the γ-ray coincidence studies using spontaneous fission of ^{252}Cf [26,27] associate the 1551-keV level with the $J^\pi = 7^-$ member of the octupole band. As a consequence, the latest ENSDF evaluation [5] introduced two energy-degenerate levels, one with $J^\pi = 5^-$ and the other with $J^\pi = 7^-$. The 1551-keV state was also observed in the present work, but based on the γ-γ coincidence information we found no evidence for the existence of the 883-keV transition, reported in Ref. [24] to feed the 4^+, 669-keV state in ^{146}Ce.

IV. DISCUSSION

The current ENSDF evaluation for ^{146}La [5] associates the 6.1-s activity with the ground state, while it associates the longer-lived 9.9-s one with the isomer. The $J^\pi = (2^-)$ and (6^-) assignments were tentatively suggested for these two states, respectively [5].

In the present work, we propose an alternative interpretation of the structure of the two β-decaying states. Since the measured spectroscopic quadrupole moments for neighboring $N = 87$–90 Ba and Cs isotopes [30–32] indicate that nuclei in this region are deformed with $\beta_2 \approx 0.15$–0.20, we invoke the Nilsson model interpretation. Systematics of experimentally observed one-quasiparticle states in ^{145}La and ^{145}Ba are shown in Fig. 5(a). The β-decay spectroscopy studies of ^{145}Ba [7,33] and spontaneous fission of ^{248}Cm [34] associate the ground state of ^{145}La with the $\pi 5/2[413]$ Nilsson orbital ($\Omega[Nn_z\Lambda]$, $\Lambda = \Omega \pm 1/2$). While no direct spin and magnetic moment measurements were performed for ^{145}La, the analysis of the in-band cascade-to-crossover branching ratios was found to be in agreement with such an interpretation [33,34]. The next orbital close to the proton Fermi surface is $\pi 3/2[411]$, which is associated with the 97.1-keV state [33]. On the neutron side, the spin of the odd-N ($N = 89$) ^{145}Ba ground state has been measured directly as $J = 5/2$ [30,31] and it was associated with the $\nu 5/2[523]$ Nilsson orbital [2]. The $\nu 1/2[530]$ orbital is assigned to the excited 175.4-keV level [35], as shown in Fig. 5(a). Following Ref. [36], the excitation energy of a given two-quasiparticle state in deformed

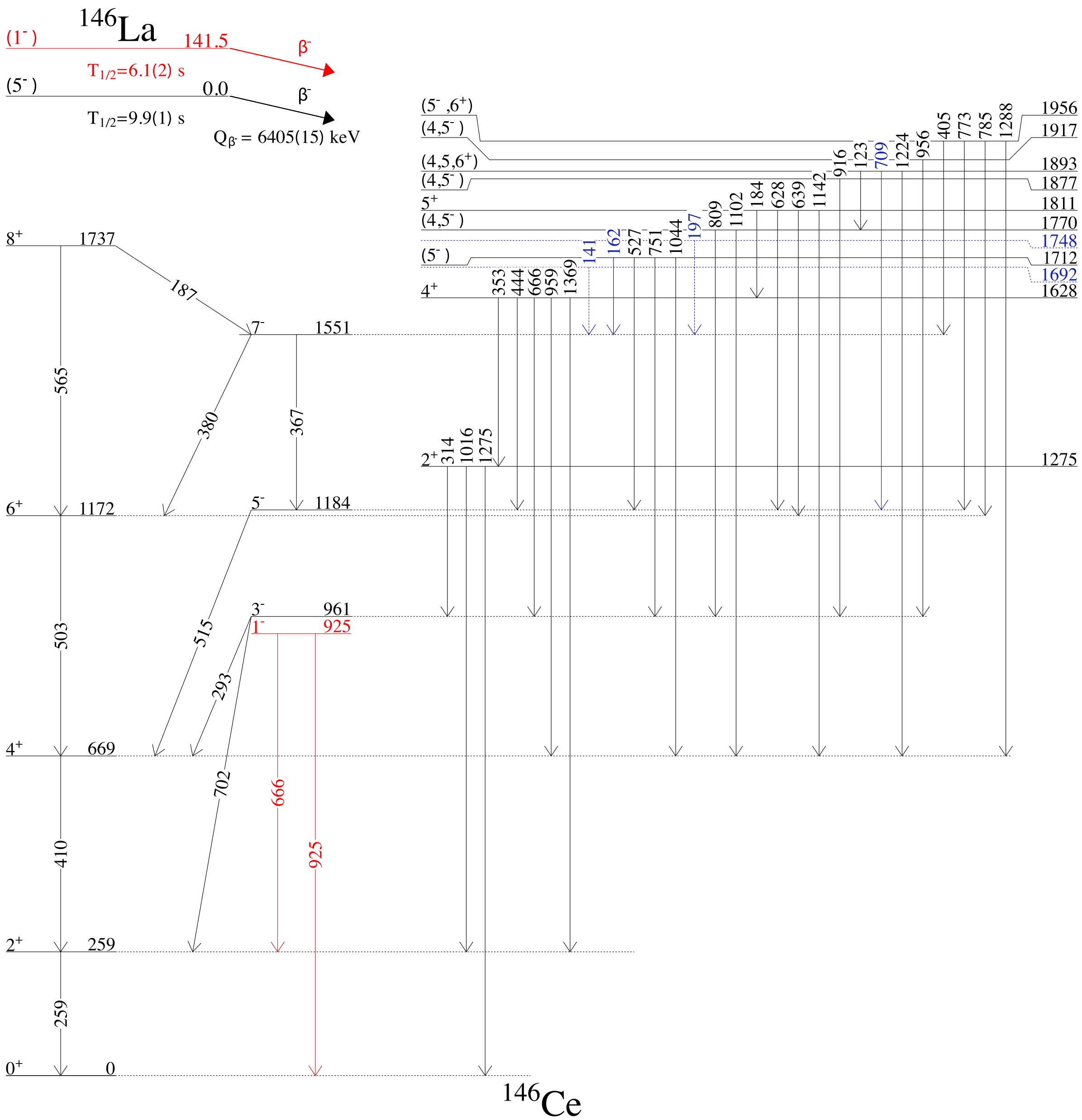

FIG. 2. Partial decay scheme of the high-spin, β-decaying state of ^{146}La, showing levels up to 1956 keV in the daughter nucleus ^{146}Ce. It was constructed using data from the CARIBU and the ^{252}Cf source experiments. The $J^{\pi} = 1^{-}$ level in ^{146}Ce is populated only from the decay of the low-spin ^{146}La isomer, and indicated in red color, together with the depopulating 666- and 925-keV γ-ray transitions. All levels and γ-ray transitions were known from previous studies [5], except those indicated in blue color, which were observed for the first time in the present work. The Q_{β} value is from Ref. [29].

odd-odd nuclei can be expressed as

$$E^{pn}_{KI} = E^{p}_{qp} + E^{n}_{qp} + a[J(J+1) - K^2] + \frac{\Delta E^{pn}_{\rm GM}}{2} + (-1)^I \left[B^{pn}_N + E^{pn}_a\right]\delta_{K,0} \quad (1)$$

where $\mathrm{E}^{p(n)}_{qp}$ is the quasiparticle energy for the odd proton (neutron), $a = \hbar^2/2\Im$ is the rotational constant, $\Im$ is the moment of inertia, $\Delta E^{pn}_{\rm GM}$ is the Gallagher-Moszkowski splitting energy, B^{pn}_N is the Newby shift and E^{pn}_a is the rotation-particle coupling term, which contributes only when $\Omega(p) = \Omega(n) = 1/2$. Following the Gallagher-Moszkowski rule [37], the sign of $\Delta E^{pn}_{\rm GM}$ is positive when the proton and neutron spins are coupled antiparallel and negative for a parallel coupling.

By combining the observed proton and neutron states in ^{145}La and ^{145}Ba and by applying Eq. (1) (for simplicity $a =$ 10 keV, corresponding to 70% of the rigid-body value of the moment of inertia, was used for all states) the lowest energy two-quasiparticle states in ^{146}La can be predicted, as shown in Fig. 5(b). The $\Delta E^{pn}_{\rm GM}$ and B^{pn}_N values for the involved Nilsson orbitals were taken from Ref. [36] using

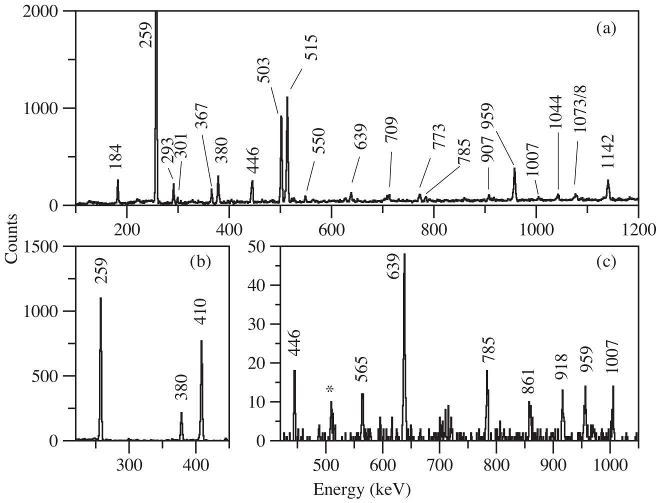

FIG. 3. Sample β-γ-γ coincidence spectra from the CARIBU experiment; (a) γ rays in coincidence with the 410-keV transition, depopulating the 4^+ level at 669 keV; (b) and (c) γ rays in coincidence with the 503-keV transition depopulating the 6^+ level at 1172 keV. The peak labeled with an asterisk corresponds to the 511-keV positron annihilation line.

the available data for the weakly deformed ^{152}Eu nucleus. As it can be seen from Fig. 5(b), the ground state of ^{146}La can be associated with the $K^\pi = 5^-$, $\pi 5/2[413]\otimes\nu 5/2[523]$ configuration, while the isomer most likely originates from the $K^\pi = 1^-$, $\pi 3/2[411]\otimes\nu 5/2[523]$ configuration, although the $K^\pi = 0^-$, $\pi 5/2[413]\otimes\nu 5/2[523]$ configuration cannot be unambiguously excluded. It is worth noting that the proposed $J^\pi = 5^-$ for the high-spin, β-decaying state in ^{146}La is in good agreement with the conclusion drawn from the observed β-decay feeding pattern, as discussed in Sec. III.

The existence of a high-spin ground state and a low-spin isomer in ^{146}La is also supported by the available mass

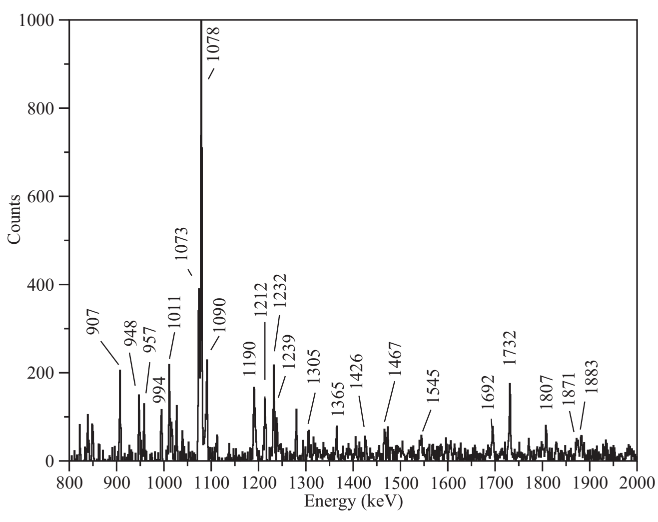

FIG. 4. Sample γ-ray coincidence spectrum from the GAMMASPHERE experiment with the stationary ^{252}Cf source produced by double gating on the 410- and 515-keV γ rays.

spectrometry data. The masses of the two β-decaying states in ^{146}La were recently measured using the CPT spectrometer [8], which were used to obtain the recommended mass-excess values of ME = −69221.1(17) keV and ME = −69079.7(17) keV [29,38], thus placing the isomer at an excitation energy of 141.5(24) keV. Unfortunately, this CPT measurement was not able to determine the ordering of the two states. However, if one considers the mass of ^{146}Ce that was measured by the CPT [39], a value of ME(^{146}Ce) = −75630(19) keV can be determined, and consequently, $Q_{\beta^-} = 6409(19)$ and 6550(19) keV for the ground state and the excited isomer in ^{146}La respectively. The end-point energy measurements associated with the shorter-lived, lower-spin β-decaying state in ^{146}La reported $Q_{\beta^-} = 6580(80)$ keV [40], 6620(70) keV [41], and 6640(50) keV (originally associated with the longer-lived state in Ref. [42], but reassigned later in Ref. [41]), which are close to the value of $Q_{\beta^-} = 6550(19)$ keV for the isomer obtained from the CPT data. Thus, the lower-spin ($T_{1/2} = 6.1$ s) β-decaying state can be associated with the isomer, while the higher-spin ($T_{1/2} = 9.9$ s) one with the ground state. This is in agreement with the proposed interpretation of the structure of the two β-decaying states in ^{146}La in the present work.

V. CONCLUSION

Excited states in ^{146}Ce were populated in β decay of the neutron-rich nucleus ^{146}La. The ^{146}La nuclei were produced by the Californium Rare Isotope Breeder Upgrade (CARIBU) facility at Argonne National Laboratory, reaccelerated by the ATLAS accelerator, and implanted on a moving-tape system in the middle of the GAMMASPHERE array, where β-delayed γ rays were measured. Additional GAMMASPHERE data obtained via fission of a standalone ^{252}Cf source, placed in the center of the array, were also used. The present data confirm the existence of two β-decaying states in ^{146}La and half-life values of 9.1(1) and 6.1(2) s were measured by tagging on specific γ rays associated with their decays. The decay scheme of the high-spin, β-decaying state in ^{146}La [$T_{1/2} = 9.1(1)$ s] was revised with respect to previous studies and evaluated nuclear data, and ambiguities that existed from previous studies were resolved. The structure of ^{146}La is discussed using the deformed Nilsson model and systematics of known quasiparticle structures in neighboring nuclei. The ground state of ^{146}La is associated with the longer-lived [$T_{1/2} = 9.1(1)$ s] state and assigned $K^\pi = 5^-$ and the $\pi 5/2[413]\otimes\nu 5/2[523]$ configuration. The isomer is proposed to originate from the $K^\pi = 1^-$, $\pi 3/2[411]\otimes\nu 5/2[523]$ configuration and it is associated with the shorter-lived [$T_{1/2} = 6.1(2)$ s] state. The ordering of the two β-decaying states in ^{146}La is also confirmed by the analysis of the available mass-spectrometry data for ^{146}La and ^{146}Ce.

ACKNOWLEDGMENTS

This work is funded by the U.S. Department of Energy, Office of Nuclear Physics, under Contracts No. DE-AC02-06CH11357 (ANL) and No. DESC0021315 (LSU), by the U.S. Department of Energy, National Nuclear Security Administration, Office of Defense Nuclear Nonproliferation

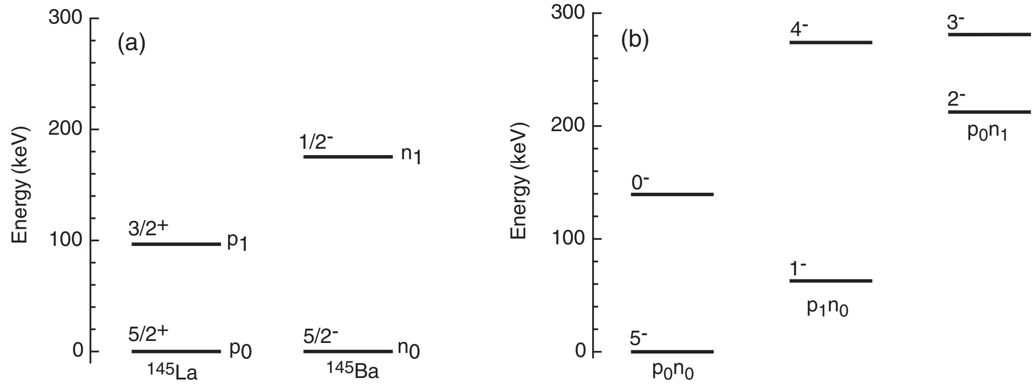

FIG. 5. (a) The experimentally observed, one-quasiparticle proton (p) and neutron (n) states in ^{145}La ($Z = 57$, $N = 88$) and ^{145}Ba ($Z = 46$, $N = 89$), respectively; p_0: $\pi 5/2[413]$ and p_1: $\pi 3/2[411]$; n_0: $\nu 5/2[523]$ and n_1: $\nu 1/2[530]$. (b) Predicted low-energy, two-quasiparticle states in ^{146}La; p_0n_0: $\pi 5/2[413] \otimes \nu 5/2[523]_{K^\pi=5^-,0^-}$, p_1n_0: $\pi 3/2[411] \otimes \nu 5/2[523]_{K^\pi=1^-,4^-}$, and p_0n_1: $\pi 5/2[413] \otimes \nu 1/2[530]_{K^\pi=2^-,3^-}$.

R&D (NA-22), by the National Science Foundation under Grant No. PHY-1502092 (USNA), by the Bulgarian National Science Fund under Contract No. KP-06-N48/1, and the European Union–Next Generation EU, the National Recovery and Resilience Plan of the Republic of Bulgaria, Project No. BG-RRP-2.004-0008-C01. S.L. acknowledges support from the Fulbright fellowship program during his stay at ANL. This research used resources of Argonne National Laboratory's ATLAS facility, which is a DOE Office of Science User Facility.

[1] W. Nazarewicz, P. Olanders, I. Ragnarsson, J. Dudek, G. A. Leander, P. Möller, and E. Ruchowska, Nucl. Phys. A **429**, 269 (1984).

[2] G. A. Leander, W. Nazarewicz, P. Olanders, I. Ragnarsson, and J. Dudek, Phys. Lett. B **152**, 284 (1985).

[3] B. Bucher, S. Zhu, C. Y. Wu, R. V. F. Janssens, D. Cline, A. B. Hayes *et al.*, Phys. Rev. Lett. **116**, 112503 (2016).

[4] B. Bucher, S. Zhu, C. Y. Wu, R. V. F. Janssens, R. N. Bernard, L. M. Robledo *et al.*, Phys. Rev. Lett. **118**, 152504 (2017).

[5] Yu. Khazov, A. Rodinov, and G. Shulyak, Nucl. Data Sheets **136**, 163 (2016).

[6] E. H. Wang, W. Lewis, C. J. Zachary, J. H. Hamilton, A. V. Ramayya, J. K. Hwang, S. H. Liu, N. T. Brewer, Y. X. Luo, J. O. Rasmussen, S. J. Zhu, G. M. Ter-Akopian, and Yu. Ts. Oganessian, Eur. Phys. J. A **53**, 234 (2017).

[7] B. Olaizola, A. Babu, R. Umashankar, A. B. Garnsworthy, G. C. Ball, V. Bildstein, M. Bowry, C. Burbadge, R. Cabellero-Folch, I. Dillmann, A. Diaz-Varela, R. Dunlop, A. Estradé, P. E. Garrett, G. Hackman, A. D. MacLean, J. Measures, C. J. Pearson, B. Shaw, D. Southall *et al.*, Phys. Rev. C **104**, 034307 (2021).

[8] R. Orford, J. A. Clark, G. Savard, A. Aprahamian, F. Buchinger, M. T. Burkey, D. A. Gorelov, J. W. Klimes, G. E. Morgan, A. Nystrom, W. S. Porter, D. Ray, and K. S. Sharma, Nucl. Instrum. Methods Phys. Res. Sect. B **463**, 491 (2020).

[9] T. Otsuka, A. Gade, O. Sorlin, T. Suzuki, and Y. Utsuno, Rev. Mod. Phys. **92**, 015002 (2020).

[10] P. A. Butler, J. Phys. G: Nucl. Part. Phys. **43**, 073002 (2016).

[11] P. A. Butler and W. Nazarewicz, Rev. Mod. Phys. **68**, 349 (1996).

[12] M. Arnould and S. Goriely, Prog. Part. Nucl. Phys. **112**, 103766 (2020).

[13] M. R. Mumpower, R. Surman, G. C. McLaughlin, and A. Aprahamian, Prog. Part. Nucl. Phys. **86**, 86 (2016).

[14] P. Dimitriou and A. L. Nichols, *Total Absorption Gamma-ray Spectroscopy for Decay Heat Calculations and other Applications*, INDC(NDS)-0676 (IAEA, Vienna, 2015).

[15] G. Savard, S. Baker, C. Davids, A. Levand, E. Moore, R. Pardo, R. Vondrasek, B. Zabransky, and G. Zinkann, Nucl. Instrum. Methods Phys. Res. Sect. B **266**, 4086 (2008).

[16] P. Copp *et al.*, (unpublished).

[17] https://gitlab.phy.anl.gov/tlauritsen/gebsort.

[18] R. Brun and F. Rademakers, Nucl. Instrum. Methods Phys. Res., Sect. A **389**, 81 (1997).

[19] D. C. Radford, Nucl. Instrum. Methods Phys. Res. Sect. A **361**, 297 (1995).

[20] E. R. Gamba, A. M. Bruce, and M. Rudigier, Nucl. Instrum. Methods Phys. Res. Sect. A **928**, 93 (2019).

[21] G. M. Gowdy, R. E. Chrien, Y. Y. Chu, R. L. Gill, H. I. Liou, M. Shmid, M. L. Stelts, K. Sistemich, F. K. Wohn, H. Yamamoto, D. S. Brenner, T. R. Yeh, R. A. Meyer, C. Chung, W. B. Walters, and R. F. Petry, in *Proceedings of the International Conference on Nuclei Far from Stability*, Helsingor, Denmark, CERN-81-09 (CERN, Geneva, 1981), Vol. I, p. 562.

[22] W. B. Walters, C. Chung, D. S. Brenner, R. Gill, M. Shmid, R. Chrien, H.-I. Liou, G. Gowdy, M. Stelts, Y. Y. Chu, F. K. Wohn, K. Sistemich, H. Yamamoto, and R. Petry, in *Proceedings of the International Conference on Nuclei Far from Stability*, Helsingor, Denmark, CERN-81-09 (CERN, Geneva, 1981), Vol. II, p. 557.

[23] A. Wolf, C. Chung, W. B. Walters, G. Peaslee, R. L. Gill, M. Shmid, V. Manzella, E. Meier, M. L. Stelts, H. I. Liou, R. E. Chrien, and D. S. Brenner, Nucl. Instrum. Methods Phys. Res. **206**, 397 (1983).

[24] T. Sharshar, S. Yamada, K. Okano, and K. Aoki, Z. Phys. A: Hadrons Nucl. **345**, 377 (1993).

[25] S. Yamada, A. Taniguchi, K. Okano, and K. Aoki, Eur. Phys. J. A **7**, 327 (2000).
[26] W. R. Phillips, R. V. F. Janssnes, I. Ahmad, H. Emling, R. Holzmann, and T. L. Khoo, Phys. Lett. B **212**, 402 (1988).
[27] J. H. Hamilton, A. V. Ramayya, S. J. Zhu, G. M. Ter-Akopian, Yu. Ts. Oganessian, J. D. Cole, J. O. Rasmussen, and M. A. Stoyer, Prog. Part. Nucl. Phys. **35**, 635 (1995).
[28] N. B. Gove and M. J. Martin, At. Data Nucl. Data Tables **10**, 205 (1971).
[29] M. Wang, W. J. Huang, F. G. Kondev, G. Audi, and S. Naimi, Chin. Phys. C **45**, 030003 (2021).
[30] A. C. Mueller, F. Buchinger, W. Klempt, E. W. Otten, R. Neugart, C. Ekström, and J. Heinemeier, Nucl. Phys. A **403**, 234 (1983).
[31] K. Wendt, S. A. Ahmad, C. Ekström, W. Klempt, R. Neugart, and E. W. Otten, Z. Phys. A **329**, 407 (1988).
[32] C. Thibault *et al.*, Nucl. Phys. A **367**, 1 (1981).
[33] M. A. Cardona, D. Hojman, B. Roussiére, I. Deloncle, N. Barre-Boscher, M. C. Mhamed, E. Cottereau, B. I. Dimitrov, G. Tz. Gavrilov, A. Gottardo, C. Lau, S. Roccia, S. Tusseau-Nenez, D. Verney, and M. S. Yavahchova, Phys. Rev. C **103**, 034308 (2021).
[34] W. Urban, W. R. Phillips, J. L. Durell, M. A. Jones, M. Leddy, C. J. Pearson, A. G. Smith, B. J. Varley, I. Ahmad, L. R. Morss, M. Bentaleb, E. Lubkiewicz, and N. Schulz, Phys. Rev. C **54**, 945 (1996).
[35] J. D. Robertson, S. H. Faller, W. B. Walters, R. L. Gill, H. Mach, A. Piotrowski, E. F. Zganjar, H. Dejbakhsh, and R. F. Petry, Phys. Rev. C **34**, 1012 (1986).
[36] A. K. Jain, R. K. Sheline, D. M. Headly, P. C. Sood, D. G. Burke, I. Hrǐvnácová, J. Kvasil, D. Nosek, and R. W. Hoff, Rev. Mod. Phys. **70**, 843 (1998).
[37] C. J. Gallagher and S. A. Moszkowski, Phys. Rev. **111**, 1282 (1958).
[38] F. G. Kondev, M. Wang, W. J. Huang, S. Naimi, and G. Audi, Chin. Phys. C **45**, 030001 (2021).
[39] G. Savard, J. C. Wang, K. S. Sharma, H. Sharma, J. A. Clark, C. Boudreau, F. Buchinger, J. E. Crawford, J. P. Greene, S. Gulick, A. A. Hecht, J. K. P. Lee, A. F. Levand, N. D. Scielzo, W. Trimble, J. Vaz, and B. J. Zabransky, Int. J. Mass Spectrom. **251**, 252 (2006).
[40] Y. Kojima, M. Shibata, H. Uno, K. Kawade, A. Taniguchi, Y. Kawase, and K. Shizuma, Nucl. Instrum. Methods Phys. Res. Sect. A **458**, 656 (2001).
[41] M. Graefenstedt, U. Keyser, F. Münnich, B. Pahlmann, B. Pfeiffer, and H. Weikard, Z. Phys. A **324**, 15 (1986).
[42] D. S. Brenner, M. K. Martel, A. Aprahamian, R. E. Chrien, R. L. Gill, H. I. Liou, M. Shmid, M. L. Stelts, A. Wolf, F. K. Wohn, D. M. Rehfield, H. Dejbakhsh, and C. Chung, Phys. Rev. C **26**, 2166 (1982).